CHEMISTRY
A EUROPEAN JOURNAL

DOI: 10.1002/chem.201102620

A Generic Platform for the Addressable Functionalisation of Electrode Surfaces through Self-Induced "Electroclick"

Christophe Orain,[a] Nicolas Le Poul,[a] Antoine Gomila,[a] Jean-Michel Kerbaol,[a] Nathalie Cosquer,[a] Olivia Reinaud,[b] Françoise Conan,[a] and Yves Le Mest*[a]

Abstract: A novel and general strategy for the immobilisation of functional objects onto electrodes is described. The concept is based on the addition of two pendant ethynyl groups onto a bis-(pyridyl)amine derivative, which acts as a molecular platform. This platform is pre-functionalised with an N_3-tagged object of interest by Huisgen cycloaddition to one of the ethynyl groups in biphasic conditions. Hence, when complexed by Cu^{II}, this molecular-object holder can be immobilised, by a "self-induced electroclick", through the second ethynyl group onto N_3-alkanethiol self-assembled monolayers on a gold electrode. Two different functional groups, a redox innocent ($(CH_2)_3$–Ph) and an electrochemical probe (ferrocene), were immobilised by following this strategy. The in situ electrochemical grafting showed, for both systems, that the kinetics of immobilisation is fast. The voltammetric characterisation of the surface-tagged functionalised copper complexes indicated that a good surface coverage was achieved and that a moderately fast electron-transfer reaction occurs. Remarkably, in the case of the redox-active ferrocenyl-immobilised system, the electrochemical response highlighted the involvement of the copper ion of the platform in the kinetics of the electron transfer to the ferrocene moiety. This platform is a promising candidate for applications in surface addressing in areas as diverse as biology and materials.

Keywords: click chemistry · copper · electrode functionalisation · N ligands · self-assembly

Introduction

The chemical functionalisation of conductive surfaces by specific molecular or biological objects is currently attracting a great deal of attention for the development of efficient devices in physical,[1] chemical[2] and biological[3] domains. Among the different strategies for immobilisation (polymeric,[4] layer-by-layer[5]), the self-assembly of monolayers (SAMs) by thiolate chemisorption on metallic surfaces is undoubtedly the most popular because it offers the advantage of yielding well-organised and controlled modified surfaces relatively easily.[6] Beyond the fundamental aspects of electron-transfer kinetics and surface self-organisation,[7–10] this approach has led to the direct immobilisation of a vast number of terminal active groups with specific properties.[6,11] However, the main drawback remains the lack of versatility. Indeed, the incorporation of a thiolated arm on to the targeted object is a prerequisite for direct grafting; this requires considerable synthetic effort and there is no guarantee that the molecules will form a structurally well-defined monolayer. Also, the immobilisation is hampered when the objects are reactive towards thiol groups, which is the case for many metallic complexes. These problems are conveniently overcome by pre-functionalisation of the electrode with reactive groups. The grafting step then operates by a chemical reaction leading to covalent binding.[6] The immobilisation of several objects, mainly of biological interest (DNA,[12] peptides,[13] carbohydrates[14]), has been successfully achieved by following this strategy.[15] However, there were some limitations as a result of the experimental conditions imposed by the chemical reaction (nucleophilic substitution, esterification, acylation, nucleophilic addition). A remarkable improvement was achieved by Collman and Chidsey and their co-workers through the adaptation of the copper-catalysed azide-alkyne cycloaddition (CuAAC "click" reaction)[16] to surface immobilisation.[17,18] Indeed, the mild conditions (room temperature) and high selectivity (1,3-cycloaddition) of this reaction are very well adapted to the modification of gold electrodes. This approach led to the surface immobilisation of several functional systems with specific properties.[19,20] Recently, Larsen and co-workers developed a procedure to selectively functionalise conducting polymers with two different alkyne-substituted fluorophores by electrochemical reduction of a Cu^{II} catalyst: the

[a] C. Orain, Dr. N. Le Poul, Dr. A. Gomila, J.-M. Kerbaol, Dr. N. Cosquer, Prof. F. Conan, Dr. Y. Le Mest
Laboratoire de Chimie, Electrochimie Moléculaire et Chimie Analytique, UMR CNRS 6521
Université de Bretagne Occidentale
6 Avenue Le Gorgeu, 29238 Brest Cedex 03 (France)
Fax: (+33) 02-98-01-70-01
E-mail: yves.lemest@univ-brest.fr

[b] Prof. O. Reinaud
Laboratoire de Chimie et de Biochimie Pharmacologique et Toxicologiques, UMR CNRS 8601
Université Paris Descartes, Sorbonne Paris Cité
45 Rue des Saint-Pères, 75006 Paris (France)

Supporting information for this article is available on the WWW under http://dx.doi.org/10.1002/chem.201102620.

"electroclick" reaction.[21] This allows spatial control of the micro-patterning of their objects. In all these examples a Cu^{I} species in solution is necessary for a heterogeneous click reaction. We recently demonstrated that electroclick onto N_3-terminated SAMs on gold could be achieved in the absence of any added copper catalyst in solution when applied to a specific copper complex with an ethynyl arm: [Cu(6-eTMPA)] (Scheme 1; 6eTMPA = 6-ethynyltris(2-pyridylmethyl)amine).[22] In our report on that work we emphasised the concept of a self-induced electroclick reaction, which allows the direct grafting of the Cu-TMPA complex in a simple electrochemical step. In this work we show that this concept can be extended to the surface immobilisation of diverse objects (R in Schemes 1 and 2). The proposed strategy is based on a two-step click modification of a so-called molecular platform in which one of the pyridine units in the 6-eTMPA ligand is replaced by an alkyne arm. The latter allows a click reaction with an N_3-tagged object R, the resulting copper complex is designed to retain the self-induced electroclick property. As shown in Scheme 2, the two-step procedure involves 1) pre-functionalisation of the platform by the object R through a chemical click reaction and 2) immobilisation of the pre-functionalised platform on an N_3-alkanethiol-modified gold electrode by a self-induced electrochemically driven click reaction in water.

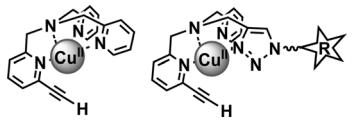

Scheme 1. Schematic representation of Cu^{II} complexes of 6-eTMPA (left) and the pre-functionalised platform (right).

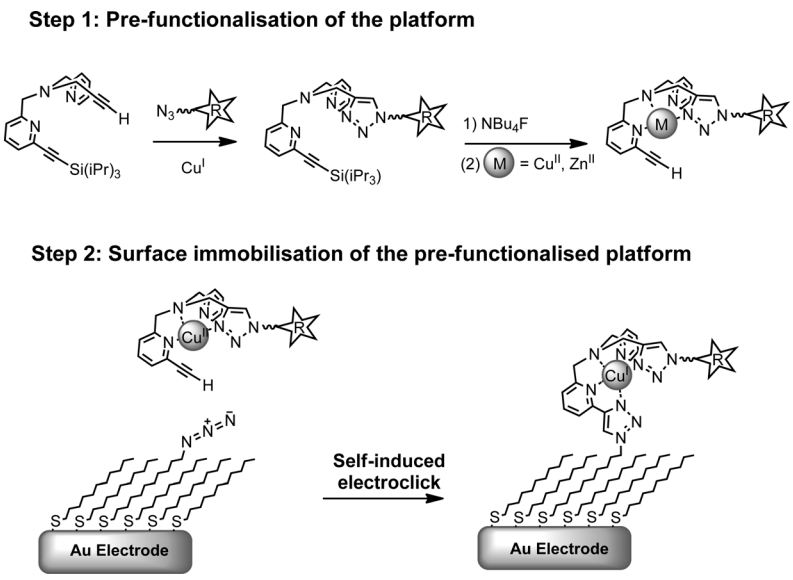

Scheme 2. Illustration of the two-step approach for the grafting of functional object R onto N_3-alkanethiol SAMs on a gold electrode.

Results and Discussion

Synthesis of the pre-functionalised platform: The platform **3** (6-TIPSe-BMPPA) was synthesised in two steps from 6-Br-BMPA (**1**) (6-Br-BMPA = (6-bromo-2-pyridylmethyl)(2-pyridylmethyl)amine; Scheme 3). In the first step, Sonogashira coupling allowed the insertion of a TIPS-protected (TIPS = triisopropylsilyl) alkyne group at the 6-position of a pyridyl group to give 6-TIPSe-BMPA (**2**; TIPSe = triisopropylsilylethynyl) in a yield of 74%. The second reaction involved a nucleophilic substitution in basic medium of the bromide group of propargyl bromide by the activated anionic form of compound **2**, which led to platform **3** (6-TIPSe-BMPPA; BMPPA = bis(2-pyridylmethyl)propargylamine) in a yield of 65%. The protection of the ethynyl arm on the pyridyl group by a TIPS group prior to the nucleophilic substitution was necessary to avoid a double-click reaction on both ethynyl groups.

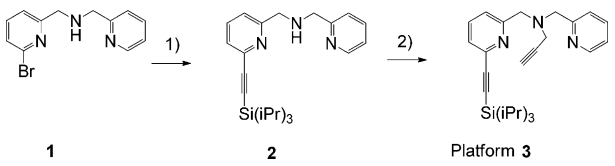

Scheme 3. Schematic pathway for the synthesis of the platform **3**: 1) (iPr)$_3$SiCCH (2 equiv), CuI (10% mol), [Pd(PPh_3)$_2$Cl$_2$] (6% mol), iPr$_2$NH/THF (1:2); 2) propargyl bromide (1.1 equiv), DIPEA (3 equiv), THF, 80°C.

Platform **3** was then pre-functionalised by a chemical CuAAC click reaction[16] under biphasic conditions (see below) to optimise product separation (Scheme 4). Thus, the organic phase (dichloromethane) containing the organosoluble compound **3** and the azido-substituted R–N_3 reactant was stirred in an aqueous solution of $CuSO_4$ (10% mol equiv) and sodium ascorbate (20% mol equiv) at room temperature for 48 h. The interfacial reaction resulted in the formation of the R-triazolo-substituted compounds **4** and **5** (R = $(CH_2)_3$–Ph and CH_2–Fc, respectively) in relatively good yields (>50%). These compounds were then treated with NBu_4F to deprotect the ethynyl arm on the pyridyl group in preparation for the electroclick reaction, which yielded compounds **6** and **7**, respectively (Scheme 4).

Complexation of the pre-functionalised platform: The coordination properties of the N_4 core

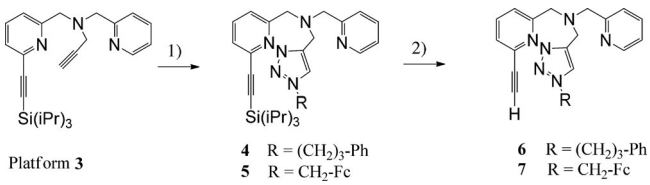

Scheme 4. Pre-functionalisation of platform **3** before the electroclick reaction: 1) $R-N_3$ (1.1 equiv), $CuSO_4$ (10% mol), Na Ascorbate (20% mol), CH_2Cl_2/H_2O (1:1); 2) NBu_4F (3 equiv), THF. Fc = ferrocene.

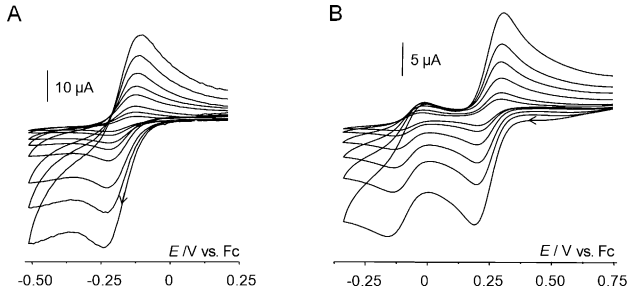

Figure 1. Cyclic voltammograms of A) [Cu(**6**)] and B) [Cu(**7**)] at a platinum electrode in CH_3CN/NBu_4PF_6 (0.1 M) under N_2 ($v = 0.02$–$2\ V\,s^{-1}$).

of the unprotected pre-functionalised platforms **6** and **7** were then explored with Cu^{II} and Zn^{II} ions. The Zn^{II} complexation of compound **7** is characterised by a ^1H NMR downfield shift of $\Delta\delta \cong 0.5$ ppm for most of its signals, which can be ascribed to the Lewis acidity and positive charge of the metal ion (Figure S1 in the Supporting Information). The complexation of ligands **6** and **7** by $Cu^{II}(OTf)_2$ yielded mononuclear complexes, which were characterised by electrochemical and spectroscopic means (Table 1).

The EPR spectra of these complexes in CH_3CN are both typical of Cu^{II} complexes with a square-pyramidal geometry ($g_{//} > g_{\perp}$), as has already been observed for $[Cu^{II}(6\text{-eTMPA})]^{2+}$ and in contrast to the bipyramidal-trigonal conformation of $[Cu^{II}(TMPA)]^{2+}$ (Figure S2).[23] In the same solvent, the [Cu(**6**)] complex is characterised by cyclic voltammetry (CV) by a single reversible system with $E° = -0.17$ V versus Fc^+/Fc at a moderate scan rate ($v = 0.1\ V\,s^{-1}$), which corresponds to the Cu^{II}/Cu^{I} redox reaction (Figure 1A). For [Cu(**7**)], two reversible systems were observed at $E° = -0.18$ and 0.14 V (Figure 1B). In rotating disk electrode voltammetry, these two systems are characterised by two successive waves of equal intensity, which indicates two one-electron exchanges. Comparison of the data for [Cu(**6**)], [Zn(**7**)] and **7** (see Table 1) shows that the process at $E° = -0.17$ V can undoubtedly be ascribed to the copper centre and the one at $E° = 0.14$ V to the ferrocene moiety.

Interestingly, the $Cu^{II/I}$ reaction occurs at a quasi-identical $E°$ value for the [Cu(**6**)] and [Cu(**7**)] complexes. This indicates that the methylferrocenyl and phenylpropyl substituents have almost the same electronic influence on the metal ion. Another remarkable point is the positive shift of $E°$ for [Zn(**7**)] and [Cu(**7**)] in comparison with free ligand **7**. This effect is likely due to electrostatic forces (charge–charge repulsion between the two metal centres in their oxidised states) and to the Lewis acidity of the zinc or copper ion, which reduces the electron density on the ferrocenyl group, as evidenced by NMR studies. In H_2O/KNO_3 (0.1 M), the CV response is different. With [Cu(**6**)] (Figure S3 in the Supporting Information), a broad reduction peak is associated with a broad reoxidation peak with a significant peak separation ($\Delta E_p \cong 600$ mV at $v = 0.1\ V\,s^{-1}$). Such behaviour is characteristic of a large reorganisation of the complex as a result of the electron-transfer reaction. In this medium, a water molecule coordinated to the Cu^{II} centre could rapidly decoordinate during the reduction to the Cu^{I} state at around $E_{pc} = -0.15$ V to produce a stable tetracoordinated cuprous species that is oxidised at around $E_{pa} = 0.45$ V versus SCE. Alternatively, a triazole or pyridine unit may undergo decoordination in the Cu^{I} oxidation state. In both cases, the Cu^{I} would be less easy to reoxidise. With [Cu(**7**)] (Figure S3 in the Supporting Information), the situation is more complicated because the sluggish oxidation peak of the electrogenerated Cu^{I} species lies in the same potential range as the ferrocene oxidation ($E_{pa} = 0.45$ V for Cu^{I} vs. $E° = 0.37$ V for Fc^+/Fc). Hence, this situation results in an intricate electron-transfer mechanism involving two almost concomitant oxidations with a possible intramolecular transfer and yields a composite peak.[24]

Table 1. EPR, Vis/NIR and electrochemical data for compounds **7**, $[Cu^{II}(\mathbf{6})]$, $[Cu^{II}(\mathbf{7})]$, $[Cu^{II}(TMPA)]$ and $[Cu^{II}(6\text{-eTMPA})]$.

Compound	Solvent	g (A [G])[a]	λ_{max} [nm] (ε [$M^{-1}cm^{-1}$])	$E°$ [V] (ΔE_p [mV])	
				Cu^{II}/Cu^{I}	Fc^+/Fc
7	CH_3CN	–	437 (167)	–	0.10 (90)[b]
$[Zn^{II}(\mathbf{7})]$	CH_3CN	–	402 (126), 718 (70)	–	0.16 (95)[b]
	H_2O				0.34 (80)[c]
$[Cu^{II}(\mathbf{6})]$	CH_3CN	$g_{//} = 2.23$ (112), $g_{\perp} = 2.06$	652 (112)	−0.17 (90)[b]	–
	H_2O			$E_{pc} = -0.15$,[c] $E_{pa} = 0.45$[c]	
$[Cu^{II}(\mathbf{7})]$	CH_3CN	$g_{//} = 2.24$ (139), $g_{\perp} = 2.06$	437 (196), 638 (103)	−0.18 (115)[d]	0.14 (90)[b]
	H_2O			$E_{pc} = -0.10$[c]	0.37 (130)[c]
$[Cu^{II}(TMPA)]$	CH_3CN	$g_{//} = 2.01$ (65), $g_{\perp} = 2.19$ (113)	889 (238), 630 (sh)[d]	−0.40 (65)[b]	–
	H_2O			−0.36 (60)[c]	
$[Cu^{II}(6\text{-eTMPA})]$[e]	CH_3CN	$g_{//} = 2.24$ (162), $g_{\perp} = 2.05$	809 (152), 640 (104)	−0.33 (65)[b]	–
	H_2O			−0.16 (120)[c]	

[a] At $T = 150$ K. [b] In CH_3CN/NBu_4PF_6 (0.1 M), E vs. Fc^+/Fc. [c] In H_2O/KNO_3 (0.1 M), $E°$ vs. SCE. [d] sh = shoulder. [e] From ref. [22].

Surface immobilisation: The [Cu^{II}(**6**)] and [Cu^{II}(**7**)] complexes were grafted onto an azidoalkanethiol-modified gold electrode by the self-induced electroclick procedure.[22] The complexes were grafted by cycling between 0.60 and −0.20 V with a 3 min hold at −0.20 V between each cycle in a 50 μM solution of [Cu(**6**)] or [Cu(**7**)] in H_2O with KNO_3 as the supporting electrolyte under an atmosphere of N_2. As shown in Figure 2A for the [Cu(**7**)] complex, the increase in the cathodic current intensity at +0.45 V (Fc) and −0.10 V (Cu) with cycling indicates that effective immobilisation of the complex has occurred on the electrode surface. After around 10 cycles, the intensity of the cathodic peaks reached a maximum value, which suggests that the maximum number of available azido sites have reacted. The shapes of the voltammetric curves, which deviate from the "ideal" behaviour (sharp oxidation peak for ferrocene, more intense than for copper), indicates that, as observed by CV in H_2O, the grafting occurs by complex mechanisms.[25] Plots of the cathodic peak intensities versus time for the ferrocenium reduction process during the immobilisation of [Cu(**7**)] allowed the kinetics of triazole formation on the surface to be estimated.

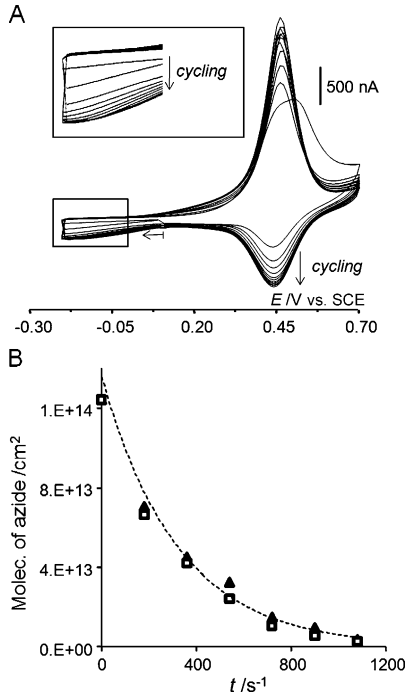

Figure 2. A) Cyclic voltammograms (10 cycles) recorded at an N_3-$(CH_2)_{11}$-SH-modified gold electrode ($v = 0.1\ V\,s^{-1}$) of [Cu(**7**)] (50 μM) in H_2O/KNO_3 (0.1 M) under N_2 with a 2 min hold at −0.20 V (Insert: variation in the cathodic current of the copper system with cycling). B) Plots of the number of available azide molecules per cm^2 vs. time for the copper (▲) and ferrocene (□) systems from the variation of cathodic peak intensities with time. Dashed line: fitted exponential curve.

As a result of the maximum surface coverage calculated from peak integration after grafting (which corresponds to the maximum number of available N_3 sites for the non-mixed modified electrode, see below), the ratio of "unclicked" available azido sites was determined for each cycle.[26] As shown in Figure 2B, the resulting decay plots display a shape that fits reasonably well with a first-order kinetic rate law (dashed line). As the reaction is bimolecular, a second-order rate constant (k) for surface immobilisation based on the Fc^+ reduction peak was calculated on the assumption that the ethynyl complex is in excess over the azido groups ($k = 160\ M^{-1}s^{-1}$). The same procedure was applied to the decrease in the peak intensity of the Cu^{II} reduction peak at −0.15 V (Figure 2, insert), taking the maximum surface coverage from peak integration after grafting (see Table 2 and Figure 3B). The good match between the second-order rate constants determined from the Fc^+ ($k = 160\ M^{-1}s^{-1}$) and Cu^{II} ($k = 180\ M^{-1}s^{-1}$) reduction peaks illustrates the validity of the process and reflects the concomitant attachment of both redox probes on to the electrode surface. The same calculation applied to [Cu(**6**)] and [Cu(6-eTMPA)] led to similar results, which attests to a fast surface reaction for these complexes with $k \cong 100\ M^{-1}s^{-1}$. Such values are, however, 10-fold lower than that found for the ferrocene-ethynyl compound described previously ($k = 1000\ M^{-1}s^{-1}$),[17c] probably for steric reasons.

Surface electrochemical characterisation: After thorough washing with distilled water, the [Cu(**6**)]- and [Cu(**7**)]-modified gold electrodes were studied in an electroactive-free sodium-acetate-buffered solution (pH 4.5; Table 2). The [Cu(**6**)]-modified electrode showed a single reversible system at $E° = 0.04$ V versus SCE (Figure 3A) with $\Delta E_p = 40$ mV at $v = 0.05\ V\,s^{-1}$ and peak intensities linearly proportional to the scan rate (not shown), which is indicative of an immobilised redox centre. The [Cu(**7**)]-modified electrode

Table 2. Electrochemical data for immobilised complexes on the modified gold electrode in $H_2O/NaBF_4$ (0.05 M)/sodium acetate (0.05 M) at pH 4.5.

Grafted complex	$E°$ [V] vs. SCE (ΔE_p [mV] at 0.05 V s^{-1})		Γ [pmol cm^{-2}]		$k°$ [s^{-1}][a]		$\Delta E_{p,1/2}$ [mV] at 0.05 V s^{-1}	
	Cu^{II}/Cu^{I}	Fc^+/Fc	Cu^{II}/Cu^{I}	Fc^+/Fc	Cu^{II}/Cu^{I}	Fc^+/Fc	Cu^{II}/Cu^{I}	Fc^+/Fc
[Cu^{II}(**6**)]	0.04 (40)	–	160[b]–110[c]	–	4	–	130	–
[Cu^{II}(**7**)]	0.04 (70)	0.42 (10)	110[b]–75[c]	160[b]–170[c]	4	90[d]	152	94
[Cu^{II}(**7**)] after dipping in NH_4OH	–	0.44 (30)	–	160[b]–140[c]	–	7	–	103
[Cu^{II}(6-eTMPA)]	−0.05 (20)	–	160[b]–90[c]	–	10	–	133	–
Fc-ethynyl	–-	0.34 (–)[e]	–	420[f]	–	500[g]	–	90–100[g]

[a] Determined from $\Delta E_p = \log v$. [b] Calculated from voltammetric peak integration at 0.05 V s^{-1}. [c] Determined from the slope $i_p = f(v)$ for $v < 0.2$ V s^{-1}. [d] Obtained from $\Delta E_p = \log v$ by using Laviron's approximation for quasi-reversible systems ($\Delta E_p < 200$ mV). [e] In 1 M $HClO_4$, E vs. Ag/AgCl/KCl (1 M) from ref. [17a]. [f] Determined for mixed monolayers from ref. [17b]. [g] Determined by chronoamperometric methods for mixed SAMs from ref. [17c].

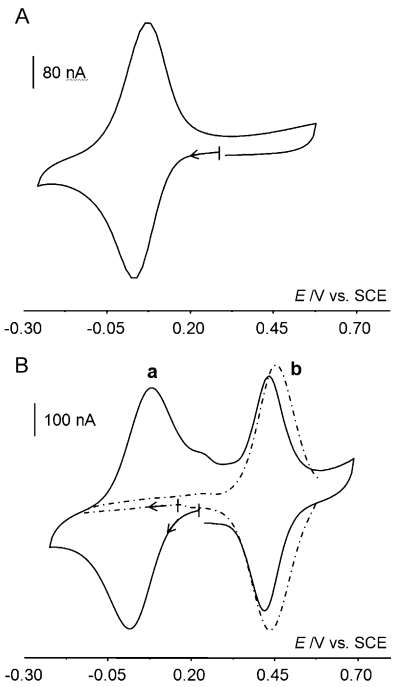

Figure 3. Cyclic voltammograms ($v=0.05\,V\,s^{-1}$) recorded in $H_2O/NaBF_4$ (0.05 M)/sodium acetate (0.05 M) at pH 4.5 under N_2 at A) a [Cu(**6**)-N_3-$(CH_2)_{11}$-SH]-modified gold electrode and B) a [Cu(**7**)-$N_3(CH_2)_{11}$-SH]-modified gold electrode a) before and b) after dipping in NH_4OH (0.01 M) for 10 min.

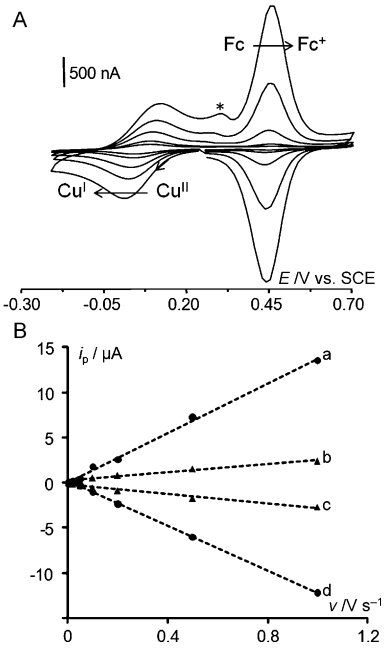

Figure 4. A) Cyclic voltammograms recorded at a [Cu(**7**)-$N_3(CH_2)_{11}$-SH]-modified gold electrode in H_2O/KNO_3 (0.1 M) under N_2 at $v=0.01$, 0.02, 0.05, 0.1 and $0.2\,V\,s^{-1}$. * See explanation in text. B) Plots of i_p vs. v ($0.02<v<1\,V\,s^{-1}$) for the ferrocenium (a and d) and copper (b and c) processes.

displayed two redox systems at $E°=0.04$ and 0.42 V versus SCE (Figure 3B, curve a), both of which are also typical of an electron-transfer reaction for an adsorbed species with a linear variation of the anodic and cathodic peak intensities with v for both systems (Figure 4). Interestingly, plots of i_p versus v for the copper and ferrocene processes yielded different slopes (smaller for copper, see Figure 4B). Also, the peak separation (ΔE_p) increased significantly with v for the Cu^{II}/Cu^{I} system, whereas it remained almost constant for ferrocene (Figure 4A and Figure 5) with a low value close to the ideal case for a very fast electron transfer to an immobilised species ($\Delta E_p=0$ mV). Such differences are ascribed to slower electron-transfer kinetics related to a reorganisational process in the $Cu^{II/I}$ reaction. Indeed, when the kinetics are no longer limiting for copper ($v<0.05\,V\,s^{-1}$), both systems display similar peak heights (Figure 3B, curve a). The increase in scan rate also led to the appearance of an extra anodic peak at around $E_{pa}=0.3$ V at $v=1\,V\,s^{-1}$ (Figure 4A, peak *); this peak potential shifts positively with increasing scan rate. As it did not appear in the first cycle when scanning positively, it can be ascribed to the oxidation of a transient Cu^{I} complex that results from the evolution of the electro-generated Cu^{I} species (EC = electrochemical-chemical mechanism). As observed by CV in solution in an aqueous medium (Figure S3 in the Supporting Information), the chemical reaction (C) following the $Cu^{II}\rightarrow Cu^{I}$ reduction step (E) might involve the release from the Cu^{I} centre of either one one pyridyl or one triazolyl arm, or an H_2O ligand (or a combination of the two processes). The fact that the same $E°$ values were found for the Cu^{II}/Cu^{I} process for both [Cu(**6**)]- and [Cu(**7**)]-modified electrodes indicates that the propylphenyl and methylferrocenyl groups have similar electronic effects on the copper centre, in agreement with previous conclusions (Table 1). To study a putative mediating effect of the copper ion on the ferrocenyl moiety, and for a better characterisation of the processes, the copper centre was removed from the [Cu(**7**)]-based immobilised electrode device by dipping it in a 0.01 M NH_4OH solution for 10 min. As shown in Figure 3B (curve b), the resulting voltammogram shows that the electrochemical signal of the Cu^{II}/Cu^{I} system has disappeared, whereas the Fc^{+}/Fc process remained almost unaffected. The surface coverage (Γ) for each modified electrode was then determined by numeric integration of the voltammetric peaks recorded at low scan rate on the basis of the geometric area ($A=0.071\,cm^2$) and from the variation of the peak current with scan rate (Table 2).[27,28] Both methods gave an average value of $\Gamma=(120\pm50)\,pmol\,cm^{-2}$, which is in the same range as that found for [Cu(6-eTMPA)] when grafted onto non-mixed azidoalkanethiol-modified gold surfaces under the same conditions (Table 2). The slight discrepancy found for the Γ values obtained for the Cu^{II}/Cu^{I} process compared with the Fc^{+}/Fc process for the [Cu(**7**)]-modified electrode indicates that the grafted complex does not follow the ideal redox behaviour expected for a monolayer with two different reversible redox systems. The higher Γ value found for the ferrocenyl centre may possibly be due to the presence of "Cu-free" tagged ferrocenyl complexes (Ø-Fc) on the surface. Another important parameter is the full-width-at-half-maxi-

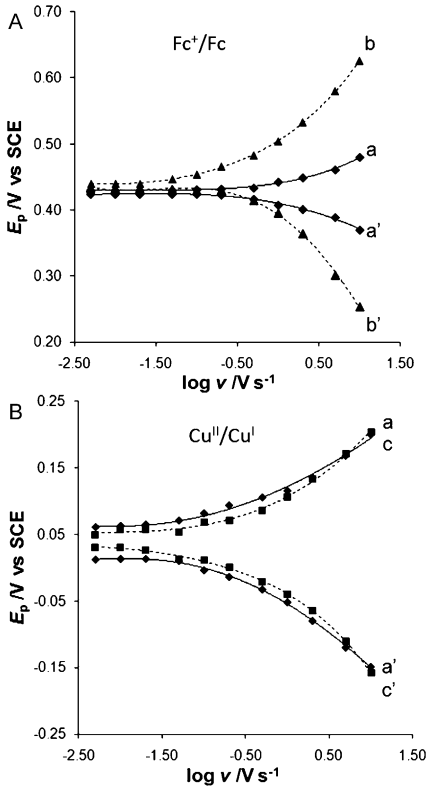

Figure 5. Plots of E_{pa} (a, b and c) and E_{pc} (a′, b′ and c′) vs. $\log v$ derived from the cyclic voltammograms of [Cu(**6**)]-, [Cu(**7**)]- and metal-free [Cu(**7**)]-modified gold electrodes in $H_2O/NaBF_4$ (0.05 M)/sodium acetate (0.05 M) at pH 4.5 under N_2 at $v = 5$–$10\ V\,s^{-1}$ for A) Fc^+/Fc and B) Cu^{II}/Cu^{I} electron-transfer processes. a,a′) The [Cu(**7**)]-modified electrode, b,b′) the metal-free [Cu(**7**)]-modified electrode prepared by dipping in NH_4OH solution and c,c′) the [Cu(**6**)]-modified electrode.

mum (fwhm) value ($\Delta E_{p,1/2}$; Table 2), which gives an indication of the deviation from the ideal reversible behaviour of an immobilised redox species (Langmuir isotherm conditions). The $\Delta E_{p,1/2}$ values obtained for the Fc^+/Fc process are close to the Nernstian case (90.6 mV at 298 K),[27,28] which suggests that the ferrocenyl groups behave as equivalent redox sites and that the global interactions between them are null. However, for the Cu^{II}/Cu^{I} process, these values are significantly higher. Such an effect may result from a combination of repulsive interactions between the copper centres and the sluggish electron-transfer kinetics, which both broadens and flattens the peaks.

Kinetics of electron transfer: The variation in the peak separation (ΔE_p) with scan rate (v) is a well-known method for determining electron-transfer kinetics between electrode-tagged species when the kinetics are not too fast ($< 10^3\ s^{-1}$). In the model developed by Laviron, in which interactions between redox centres are not considered, the standard rate constant $k°$ is calculated from the intercept of the linear part of the peak separation ΔE_p versus $\log v$ ($\Delta E_p > 200$ mV for a one-electron-transfer reaction).[29] This allowed $k°$ values to be evaluated for [Cu(**6**)] and [Cu(**7**)] complexes (Figure 5 and Table 2). The calculations show that the $Cu^{II/I}$ electron-transfer process is moderately fast ($4\ s^{-1}$) irrespective of the nature of the substituting group (Fc or Ph). They are also of the same order of magnitude as that found for the grafted [Cu(6-eTMPA)] complex measured under similar conditions ($10\ s^{-1}$). Remarkably, for the Fc^+/Fc process, the peak separation depends on whether or not the copper centre is present, as clearly depicted in Figure 5A. Indeed, the calculations give a standard rate constant of $7\ s^{-1}$ for the tagged metal-free [Cu(**7**)] complex. When copper is present, the electron transfer is significantly faster ($k° = 90\ s^{-1}$) and is closer to the value found for the ethynylferrocene complex grafted on undecanethiol chains ($500\ s^{-1}$).[17c,30] Two main effects may explain the key role of the copper ion on the kinetics. The first is the structural stiffening of the tagged complex in the presence of copper through the formation of coordinating bonds between the metal ion and N-donor groups (two pyridyl, two triazoles, one amine). This induces a decrease in the distance separating the ferrocenyl moiety from the electrode surface, as depicted in Scheme 5. Consequently, the electron transfer between the electrode and the ferrocenyl moiety is substantially accelerated.[31] A second possible explanation is that the copper complex acts as an electron relay in the electron-hopping process from the electrode to the ferrocene. The presence of the metal ion would induce a sequential localisation of the charge and a decrease in the activation energy for the whole electron transfer. However, this second hypothesis is unlikely in the case of [Cu(**7**)]: the standard potentials of the Cu^{II}/Cu^{I} and Fc^+/Fc processes are not close enough to each other ($\Delta E° = 380$ mV) to allow a self-exchange mechanism by electron hopping. In fact, charge-hopping processes in SAMs have rarely been described in the literature[32] because most of the studies have been per-

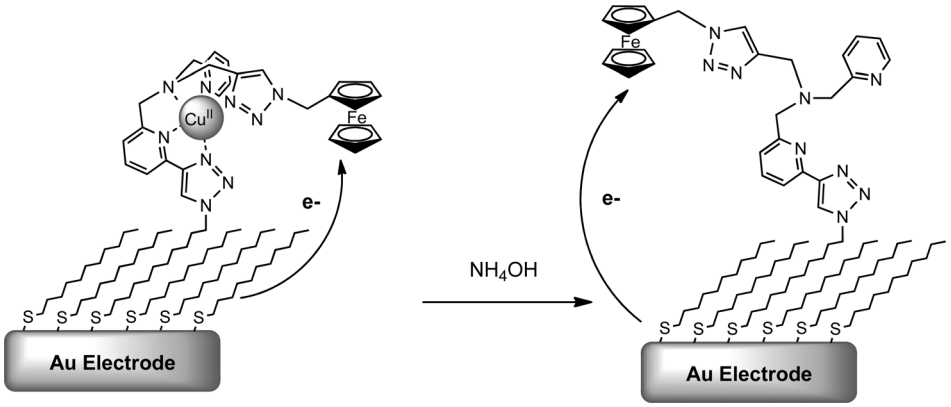

Scheme 5. Hypothesis for the difference in electron-transfer kinetics for the [Cu(**7**)]-modified electrode before and after copper removal by a NH_4OH treatment.

formed with mono-functional systems with saturated or unsaturated chains.

Conclusion

Two main strategies have classically been used for the functionalisation of a surface. The most straightforward approach is the direct grafting of the object of interest, which, however, has two problems. It is restricted to compounds presenting a reactive moiety towards the surface; this raises the difficulty of functional compatibility with that of the compound itself. Also, it can hardly insure good covering of the surface, that is, impermeability to direct electron transfer when the compound cannot be packed as a dense monolayer due to steric crowding. The second strategy involves a two-step procedure: functionalisation of the surface with an alkyne (generally a thiol) or an aryl (e.g., a diazo) with a function that will, in the second step, react with the compound of interest. The most popular reaction used for this second step is the CuAAC procedure, which requires the use of a copper catalyst.

We have proposed in this work a novel and versatile strategy that involves the use of a generic molecular platform (compound **3**). This platform was designed to provide two sequentially addressable moieties: one for the object to graft, the other for the pre-functionalised electrode. The key point of our strategy is the formation, after the first click reaction, of an N_4 ligand bound to the object. The subsequent stoichiometric N_4 complexation of Cu^{II} allows the object of interest to be connected to the pre-functionalised surface directly by a simple self-induced electroclick reaction. The advantages of such a strategy based on platform **3** are multiple: 1) the grafting step is electrochemically addressable, 2) it is easily monitored and quantified, 3) the grafting procedure is "clean" as no exogenous copper complex is required, 4) each reaction employed in the multistep strategy is high yielding and has a high chemical tolerance and finally 5) the formation of the intermediate Cu^{II} complex increases the hydrophilicity of the object and thus its solubility in water, a key solvent for avoiding the denaturation of the alkynethiol monolayer. This last point is particularly interesting for the grafting of organic substrates that are poorly water soluble. As a proof of concept, two different functional groups were immobilised to evaluate this strategy, a redox-innocent phenyl group and a redox probe, ferrocene. Monitoring of the in situ electrochemical grafting showed that the kinetics of immobilisation is fast for both systems with good surface coverage. Remarkably, also, the study of the ferrocenyl-based copper complex highlighted the influence of the copper ion on the kinetics of electron transfer to ferrocene by combined structural/electronic effects. Hence the molecular platform **3** appears to be a promising candidate for applications in surface addressing in areas ranging from electronics to biology. Indeed, it addresses two issues: First, the possibility of selective surface patterning through electrochemical control; this has been demonstrated in the case of a gold electrode but should be extendable to the more robust vitreous and graphitic electrodes.[33,34] Secondly, thanks to the presence of the N_4–Cu redox link, it allows electron communication between two different probes to be explored. Indeed, the experimental evidence for electron relay in molecular devices is of great interest in biology (e.g., a model for electron-transfer in DNA[35]) and biotechnology (design of new biochips[]).[36] We are currently working on these two aspects.

Experimental Section

Chemicals: Organic solvents were distilled over CaH_2 except for THF and diethyl ether which were distilled over Na/benzophenone. Acetonitrile (99.9% BDH, VWR) was used as received and kept under N_2 in a glovebox. All solvents were thoroughly degassed before use. NBu_4PF_6 was synthesised from NBu_4OH (Fluka) and HPF_6 (Aldrich). It was then purified, dried under vacuum for 48 h at 100 °C and then stored under N_2 in the glovebox. Compounds 6-Br-BMPA,[37] $FcCH_2N_3$[38] and $Ph(CH_2)_2N_3$[39] were prepared according to literature procedures. 11-Azidoundecane-1-thiol was synthesised following a previously described procedure.[17a] All other chemicals were of reagent grade and were used without purification.

Apparatus: NMR spectra were recorded on a Bruker DRX 500 MHz spectrometer. IR spectra were recorded on a Nicolet Nexus FT-IR spectrometer (KBr pellets). EPR spectra were recorded on a Bruker Elexys spectrometer (X band). UV/Vis/NIR spectroscopy was performed with a JASCO V-670 spectrophotometer. Single-mass analyses were performed by the Service Central d'Analyse du CNRS, Solaize, France.

Electrochemical experiments: The electrochemical studies in acetonitrile were performed in a glovebox (Jacomex, $O_2 < 1$ ppm, $H_2O < 1$ ppm) with a home-designed 3-electrode cell. A commercial platinum removable tip electrode (Metrohm) was used as the working electrode. Before each experiment, it was polished in a slurry of alumina (3 μm) and sonicated in water (Millipore, 18 MΩ). The counter electrode was a platinum wire. A separate frit containing a platinum electrode dipped in an equimolar electrolytic solution of $FcPF_6$ and ferrocene was used as the reference electrode. The potential of the cell was controlled by an AUTOLAB PGSTAT 302 (Ecochemie) potentiostat monitored with a computer piloted with GPES software. Ferrocene was added at the end of each experiment to determine accurate redox potentials. Voltammetry was performed in an aqueous electrolyte with a standard calomel reference electrode (saturated KCl) as reference.

Electrode modification: A commercial gold removable tip electrode (Metrohm) was used. Before modification, the surface of the gold electrode ($A = 0.071\ cm^2$) was prepared following a classical procedure by polishing in a slurry with alumina (3 μm). It was then sonicated in water (Millipore, 18 MΩ) and cycled between +0.5 and 1.4 V versus SCE in 0.1 M H_2SO_4 (40 scans) to remove gold oxide, washed with water, then ethanol and dried under a slow flow of N_2 before being introduced into a solution containing thiol. This procedure allowed the use of the same electrode with a renewed appropriate gold surface condition. The electrode was kept in a non-mixed 1 mM 1-azido-11-undecanethiol solution in EtOH for 12 h under N_2. After thorough washing with pure EtOH, the electrode was tested by voltammetry in an aqueous solution of ferricyanide. The absence of a redox signal indicated a blockage of electron transfer at the electrode surface by the thiol compound.

Synthesis of 2: 6-Br-BMPA (1.80 mmol, 500 mg) was dissolved in a degassed THF/diisopropylamine mixture (2:1 v/v). Under N_2, CuI (0.18 mmol, 35 mg), $[Pd(PPh_3)_2Cl_2]$ (0.11 mmol, 76 mg) and finally triisopropylacetyene (3.6 mmol, 0.80 mL) were added. The reaction mixture was stirred for 16 h at room temperature. The solution was filtered and the solid washed with THF (3×25 mL). The solvent was removed with a rotary evaporator, the black oil obtained was dissolved in CH_2Cl_2

(50 mL) and washed with water (5×30 mL). The organic phase was dried over $MgSO_4$, filtered through hydrophilic cotton and the solvent was removed with a rotary evaporator. The product was isolated in a yield of 74% (508 mg, 1.34 mmol) by alumina column chromatography with CH_2Cl_2/MeOH (99:1). ^{1}H NMR (300 MHz, $CDCl_3$): δ=8.56 (d, J=4.5 Hz, 1H), 7.69–7.33 (m, 5H), 7.15 (dd, J=4.5, 1 Hz, 1H), 3.98 (s, 4H), 2.71 (br s, 1H), 1.16 ppm (m, 21H).

Synthesis of 3: 6-TIPSe-BMPA (1.34 mmol, 508 mg) was dissolved in THF (20 mL). Under an inert atmosphere, propargyl bromide (1.47 mmol, 0.15 mL, 80% in toluene) and DIPEA (4 mmol, 0.70 mL) were added. The reaction mixture was heated at reflux overnight. The solution was filtered and the solid washed three times with THF (25 mL). The solvent was removed with a rotary evaporator. The product was dissolved in CH_2Cl_2 (90 mL), washed with water (3×50 mL), dried over $MgSO_4$, filtered through cotton and the solvent was removed with a rotary evaporator. The product was purified by column chromatography on silica gel with CH_2Cl_2/MeOH as eluent (99:1), to give a yield of 65%. ^{1}H NMR (500 MHz, $CDCl_3$): δ=8.49 (d, J=4.8 Hz, 1H), 7.59 (t, J=7.7 Hz, 1H), 7.55 (t, J=7.5 Hz, 1H), 7.47 (d, J=7.5 Hz, 1H), 7.44 (d, J=7.8 Hz, 1H), 7.29 (d, J=7.3 Hz, 1H), 7.09 (dd, J=7.3, 4.9 Hz, 1H), 3.88 (s, 2H), 3.85 (s, 2H), 3.37 (d, J=2.3 Hz, 2H), 2.24 (t, J=2.3 Hz, 1H), 1.11 ppm (m, 21H); ^{13}C NMR (500 MHz, $CDCl_3$): δ=159.6, 159.1, 149.1, 142.2, 136.3, 126.34, 123.0, 121.9, 107.32, 91.4, 77.8, 73.0, 59.1, 59.0, 43.4, 18.5, 11.2 ppm; IR (KBr): $\tilde{\nu}$=3306 (m), 3058 (m), 2943 (s), 2865 (s), 2157 (m, $\tilde{\nu}$C≡C–Si), 2103 (w, $\tilde{\nu}$C≡C–H) 1683 (m), 1581 (s), 1569 (s), 1447 (s), 1267 (m), 1120 (m), 996 (s), 883 (s), 734 (m), 678 cm^{-1} (s); MS (TOF ES+, MeOH): m/z: calcd for $C_{26}H_{36}N_3Si$ $[M+H]^+$: 418.2679; found: 418.2683.

General procedure for the synthesis of compounds 4 and 5: 6-TIPSe-BMPPA (**3**) and 1-azido-3-phenylpropane (for **4**) or azidomethylferrocene (**5**) in a 1:1 ratio were added to a solution of dichloromethane (15 mL). Aqueous solutions of $CuSO_4$·$5H_2O$ (0.1 mol equiv, 7.5 mL) and sodium ascorbate (0.2 mol equiv, 7.5 mL) were prepared. Then the three solutions were combined (gathered) and stirred vigorously for 48 h under an inert atmosphere at room temperature. Dichloromethane and water (50 mL of each) were added to the mixture. The aqueous phase was extracted with CH_2Cl_2 (2×50 mL) and the organic phases were collected, washed with water (3×75 mL), dried over $MgSO_4$ and filtered through cotton. The solvent was removed with a rotary evaporator.

Purification and characterisation of 4: Compound **4** was purified by column chromatography on silica gel with CH_2Cl_2/MeOH as eluent (methanol ratio from 0 to 1.5% v/v). The yellow product was obtained in a yield of 45%. ^{1}H NMR (500 MHz, $CDCl_3$): δ=8.55 (d, J=3 Hz, 1H), 7.66–7.56 (m, 4H), 7.36 (dd, J=7.5, 1 Hz, 1H), 7.31 (m, 2H), 7.21–7.15 (m, 4H), 4.34 (t, J=7 Hz, 2H), 3.89 (s, 2H), 3.87 (s, 2H), 3.84 (s, 2H), 2.65 (t, J=7.5 Hz, 2H), 2.25 (q, J=7.5 Hz, 2H), 1.16 ppm (m, 21H).

Characterisation of 5: Compound **5** was used in the next step without additional purification. ^{1}H NMR (400 MHz, $CDCl_3$): δ=8.50 (d, J=4 Hz, 1H), 7.62–7.53 (m, 5H), 7.32 (d, J=8 Hz, 1H), 7.12 (dd, J=4.6 Hz, 1H), 5.24 (s, 2H), 4.25 (s, 2H), 4.19 (s, 2H), 4.16 (s, 5H), 3.83 (s, 2H), 3.81 (s, 2H), 3.80 (s, 2H), 1.14 ppm (m, 21H).

General procedure for the synthesis of compound 6 and 7: Compound **4** or **5** was dissolved in THF (20 mL) and NBu_4F (3 mol equiv) was added to the solution. The reaction mixture was stirred for 15 h and then THF was removed with a rotary evaporator. The product was dissolved in CH_2Cl_2 (50 mL) and extracted with an aqueous solution of 0.5 M HCl (3×50 mL). The aqueous phase was collected and the pH adjusted to 8.6. CH_2Cl_2 (100 mL) was added and reaction mixture was vigorously stirred for 30 min. Then the aqueous phase was extracted with CH_2Cl_2 (2×75 mL). The organic phases were collected and washed with water (2×100 mL), dried over $MgSO_4$, filtered through cotton and the solvent removed with a rotary evaporator.

Purification and characterisation of 6: Compound **6** was purified by column chromatography on silica gel with CH_2Cl_2/MeOH as eluent (99:1), to give the product in a yield of 65%. ^{1}H NMR (500 MHz, $CDCl_3$): δ=8.53 (d, J=5 Hz, 1H), 7.67–7.55 (m, 4H), 7.33 (dd, J=6, 3 Hz, 1H), 7.28–7.25 (m, 2H), 7.19–7.14 (m, 4H), 4.31 (t, J=7 Hz, 2H), 3.90 (s, 2H), 3.88 (s, 2H), 3.87 (s, 2H), 3.11 (s, 1H), 2.61 (t, J=7.5 Hz, 2H), 2.21 ppm (q, J=7.25 Hz, 2H); ^{13}C NMR (500 MHz, $CDCl_3$): δ=159.4, 158.3, 148.8, 143.5, 141.4, 140.1, 136.7, 128.6–128.3, 126.3, 125.9, 123.4, 122.3, 82.8, 59.2, 49.4, 48.6, 32.5, 31.6 ppm; MS (TOF ES+, MeOH): m/z: calcd for $C_{26}H_{27}N_6$ $[M+H]^+$: 423.2297; found: 423.2304.

Purification and characterisation of 7: Compound **7** was purified by column chromatography on silica gel with CH_2Cl_2/MeOH as eluent (methanol ratio from 0 to 3% v/v). The dark-red product was obtained in a yield of 51%. This yield is for the click reaction and deprotection procedure. ^{1}H NMR (500 MHz, $CDCl_3$): δ=8.52 (d, J=4 Hz, 1H), 7.65–7.61 (m, 5H), 7.34 (m, 1H), 7.14 (dd, J=4, 5.5 Hz, 1H), 5.27 (s, 2H), 4.27 (s, 2H), 4.20 (s, 2H), 4.17 (s, 5H), 3.87 (s, 6H), 3.13 ppm (s, 1H); ^{13}C NMR (500 MHz, $CDCl_3$): δ=160, 159, 148.9, 144, 141.4, 136.8, 126.0, 123.7, 123.4, 122.9, 122.3, 28.9, 81.1, 69.0, 59.3, 50.0, 48.8 ppm; MS (TOF ES+, MeOH): m/z: calcd for $C_{28}H_{27}N_6Fe$ $[M+H]^+$: 503.1647; found: 503.1654.

Acknowledgements

This project was supported by the CNRS (Institut de Chimie), the Ministère de l'Enseignement Supérieur et de la Recherche (MESR Ph.D. grant to C.O.) and Agence Nationale pour la Recherche (Cavityzyme(Cu) Project ANR-2010-BLAN-7141).

[1] a) A. Pron, P. Gawrys, M. Zagorska, D. Djurado, R. Demadrillea, *Chem. Soc. Rev.* **2010**, *39*, 2577–2632; b) M. Grätzel, *Inorg. Chem.* **2005**, *44*, 6841–6851; c) B. Ulgut, H. D. Abruna, *Chem. Rev.* **2008**, *108*, 2721–2736.

[2] a) J. Chen, W. Zhang, D. Officer, G. F. Swiegers, G. G. Wallace, *Chem. Commun.* **2007**, 3353–3355; b) I. Willner, E. Katz, *Angew. Chem.* **2000**, *112*, 1230–1269; c) L. Shen, Z. Chen, Y. Li, S. He, S. Xie, X. Xu, Z. Liang, X. Meng, Q. Li, Z. Zhu, M. Li, X. C. Le, Y. Shao, *Anal. Chem.* **2008**, *80*, 6323–6328; d) D. Nkosi, J. Pillay, K. I. Ozoemena, K Nouneh, M. Oyama, *Phys. Chem. Chem. Phys.* **2010**, *12*, 604–613; e) E. Bakker, Y. Qin, *Anal. Chem.* **2006**, *78*, 3965–3983.

[3] J. A. Cracknell, K. A. Vincent, F. A. Armstrong, *Chem. Rev.* **2008**, *108*, 2439–2461.

[4] a) A. Heller, *Curr. Opin. Chem. Biol.* **2006**, *10*, 664–672; b) C. Bunte, O. Prucker, T. König, J. Rühe, *Langmuir* **2010**, *26*, 6019–6027; c) B. A. Gregg, A. Heller, *J. Phys. Chem.* **1991**, *95*, 5976–5980; d) S. Cosnier, *Biosens. Bioelectron.* **1999**, *14*, 443–456.

[5] a) G. Decher, *Science* **1997**, *277*, 1232–1237; b) J. Hodak, R. Etchenique, E. J. Calvo, K. Singhal, P. N. Bartlett, *Langmuir* **1997**, *13*, 2708–2716; c) V. Flexer, E. S. Forzani, E. J. Calvo, S. J. Luduena, L. I. Pietrasanta, *Anal. Chem.* **2006**, *78*, 399–407.

[6] J. C. Love, L. A. Estroff, J. K. Kriebel, R. G. Nuzzo, G. M. Whitesides, *Chem. Rev.* **2005**, *105*, 1103–1169.

[7] a) C. E. D. Chidsey, C. R. Bertozzi, . T. M. Putvinski, A. M. Mujsce, *J. Am. Chem. Soc.* **1990**, *112*, 4301–4306; b) C. E. D. Chidsey, *Science* **1991**, *251*, 919–922.

[8] C. Amatore, S. Gazard, E. Maisonhaute, C. Pebay, B. Schöllhorn, J.-L. Syssa-Magalé, J. Wadhawan, *Eur. J. Inorg. Chem.* **2007**, 4035–4042.

[9] a) J. Sumner, S. E. Creager, *J. Phys. Chem. B.* **2001**, *105*, 8739–8745; b) H. O. Finklea, D. D. Hanshaw, *J. Am. Chem. Soc.* **1992**, *114*, 3173–3181; c) D. A. Brevnov, H. O. Finklea, H. Van Ryswyk, *J. Electroanal. Chem.* **2001**, *500*, 100–107; d) L. Tender, M. T. Carter, R. W. Murray, *Anal. Chem.* **1994**, *66*, 3173–3181.

[10] a) O. Alévêque, P.-Y. Blanchard, C. Gautier, M. Dias, T. Breton, E. Levillain, *Electrochem. Commun.* **2010**, *12*, 1462–1466; b) S. J. Green, N. Le Poul, P. P. Edwards, G. Peacock, *J. Am. Chem. Soc.* **2003**, *125*, 3686–3687.

[11] a) A. L. Eckermann, D. J. Feld, J. A. Shaw, T. J. Meade, *Coord. Chem. Rev.* **2010**, *254*, 1769–1802; b) E. Tran, M. A. Rampi, G. M.

Whitesides, *Angew. Chem.* **2004**, *116*, 3923–3927; *Angew. Chem. Int. Ed.* **2004**, *43*, 3835–3839.
[12] a) B. T. Houseman, E. S. Gawalt, M. Mrksich, *Langmuir* **2003**, *19*, 1522–1531; b) E. A. Smith, W. D. Thomas, Y. Cheng, S. V. P. Barreira, A. G. Frutos, R. M. Corn, *Langmuir* **2001**, *17*, 2502–2507.
[13] G. J. Wegner, H. J. Lee, R. M. Corn, *Anal. Chem.* **2002**, *74*, 5161–5168.
[14] E. A. Smith, W. D. Thomas, L. L. Kiessling, R. M. Corn, *J. Am. Chem. Soc.* **2003**, *125*, 6140–6148.
[15] The immobilisation of redox proteins onto thioalkane-modified electrodes is not considered here as they specifically bind through non-covalent modes. See, for example: M. J. Tarlov, E. F. Bowden, *J. Am. Chem. Soc.* **1991**, *113*, 1847–1849.
[16] V. V. Rostovtsev, L. G. Green, V. V. Fokin, K. B. Sharpless, *Angew. Chem.* **2002**, *114*, 2708–2711; *Angew. Chem. Int. Ed.* **2002**, *41*, 2596–2599.
[17] a) J. P. Collman, N. K. Devaraj, C. E. D. Chidsey, *Langmuir* **2004**, *20*, 1051–1053; b) J. P. Collman, N. K. Devaraj, T. P. A. Eberspacher, C. E. D. Chidsey, *Langmuir* **2006**, *22*, 2457–2464; c) N. K. Devaraj, R. A. Decreau, W. Ebina, J. P. Collman, C. E. D. Chidsey, *J. Phys. Chem. B.* **2006**, *110*, 15955–15962.
[18] N. K. Devaraj, P. H. Dinolfo, C. E. D. Chidsey, J. P. Collman, *J. Am. Chem. Soc.* **2006**, *128*, 1794–1795.
[19] J. P. Collman, N. K. Devaraj, R. A. Decreau, Y. Yang, Y.-L. Yan, W. Ebina, T. A. Eberspacher, C. E. D. Chidsey, *Science* **2007**, *315*, 1565–1568.
[20] a) N. K. Devaraj, G. P. Miller, W. Ebina, B. Kakaradov, J. P. Collman, E. T. Kool, C. E. D. Chidsey, *J. Am. Chem. Soc.* **2005**, *127*, 8600–8601; b) Y. Zhang, S. Luo, Y. Tang, L. Yu, K.-Y. Hou, J.-P. Cheng, X. Zeng, P. G. Wang, *Anal. Chem.* **2006**, *78*, 2001–2008; c) J. F. Lutz, *Angew. Chem.* **2007**, *119*, 1036–1043; *Angew. Chem. Int. Ed.* **2007**, *46*, 1018–1025.
[21] T. S. Hansen, A. E. Daugaard, S. Hvilsted, N. B. Larsen, *Adv. Mater.* **2009**, *21*, 4483–4486.
[22] A. Gomila, N. Le Poul, N. Cosquer, J.-M. Kerbaol, J.-M. Noël, M. T. Reddy, I. Jabin, O. Reinaud, F. Conan, Y. Le Mest, *Dalton Trans.* **2010**, *39*, 11516–11518.
[23] N. Le Poul, B. Douziech, J. Zeitouny, G. Thiabaud, H. Colas, F. Conan, N. Cosquer, I. Jabin, C. Lagrost, P. Hapiot, O. Reinaud, Y. Le Mest, *J. Am. Chem. Soc.* **2009**, *131*, 17800–17808.
[24] The exact nature of the mechanism has not been scrutinised due to the instability of the compounds in aqueous media and problems of insolubility and deposition at the surface of the electrode.
[25] A similar voltammetric shape (but no increase in the peak intensities) was obtained when cycling with the same solution, but without holding the potential at −0.20 V for an azido-modified gold electrode. This clearly indicates that the ferrocene moiety of the complex can diffuse into the azidoundecanethiol monolayer, which is no longer "insulating". Such mass-transfer processes may thus be responsible for the appearance of the sharp oxidation peak observed with higher current intensities for ferrocene during grafting, similarly to what is observed in solution.
[26] The theoretical surface coverage of optimally well-packed alkanethiols on Au(111) is 775 pmol cm^{-2} (see ref. [17b]). The experimental surface coverage of the complex from Fc peak integration at 0.05 V s^{-1} is 160 pmol cm^{-2}, that is, 20% of the theoretical value. Such a discrepancy, which has been mentioned by Chidsey and coworkers,[17b] is due to the steric limitation inherent to the size of the ethynyl substrate (in the case of ethynylferrocene, a maximum value of 55% was found[17b]).
[27] A. J. Bard, L. R. Faulkner, *Electrochemical Methods: Fundamentals and Applications*, 2nd ed., John Wiley & Sons, New York, **2001**, pp. 580–631.
[28] J.-M. Savéant, *Elements of Molecular and Biomolecular Electrochemistry*, John Wiley & Sons, Hoboken, **2006**, pp. 1–77.
[29] E. Laviron, *J. Electroanal. Chem.* **1979**, *101*, 19–28.
[30] The calculation of the standard rate constant for the Fc^+/Fc system for the [Cu(**7**)]-modified electrode was performed by using Laviron's procedure for quasi-reversible systems ($\Delta E_p < 200$ mV).[29]
[31] The rate of electron transfer falls exponentially with the distance from the saturated alkane chains, see refs. [7,9].
[32] C. Amatore, E. Maisonhaute, B. Schöllhorn, J. Wadhawan, *ChemPhysChem* **2007**, *8*, 1321–1329.
[33] D. Evrard, F. Lambert, C. Policar, V. Balland, B. Limoges, *Chem. Eur. J.* **2008**, *14*, 9286–9291.
[34] C. C. L. McCrory, A. Devadoss, X. Ottenwaelder, R. D. Lowe, T. D. Stack, C. E. D. Chidsey, *J. Am. Chem. Soc.* **2011**, *133*, 3696–3699.
[35] a) B. Giese, M. Spichty, *ChemPhysChem* **2000**, *1*, 195–198; b) G. B. Schuster, *Acc. Chem. Res.* **2000**, *33*, 253–260.
[36] E. M. Boon, D. M. Ceres, T. G. Drummond, M. G. Hill, J. K. Barton, *Nat. Biotechnol.* **2000**, *18*, 1096–1100.
[37] M. Merkel, D. Schnieders, S. M. Baldeau and B. Krebs, *Eur. J. Inorg. Chem.* **2004**, 783–790.
[38] J. M. Casas-Solvas, A. Vargas-Berenguel, L. F. Capitan-Vallvey, F. Santo-Gonzalez, *Org. Lett.* **2004**, *6*, 3687–3690.
[39] G. Colombano, C. Travelli, U. Galli, A. Caldarelli, M. G. Chini, P. L. Canonico, G. Sorba, G. Bifulco, G. C. Tron, A. A. Genazzani, *J. Med. Chem.* **2010**, *53*, 616–623.

Received: August 23, 2011
Published online: December 9, 2011

